Journal of Materials Chemistry A

Superhydrophobic and Stable Mesoporous Polymeric Adsorbent for Siloxane Removal: D4 Super-Adsorbent

Journal:	*Journal of Materials Chemistry A*
Manuscript ID:	TA-ART-12-2014-006593.R1
Article Type:	Paper
Date Submitted by the Author:	12-Jan-2015
Complete List of Authors:	Jafari, Tahereh; University of connecticut, Institute of Material Science Noshadi, Iman; Harvard-MIT Health Sciences and Technology, Khakpash, Nasser; University of Connecticut, Department of Material Science and Engineering and Institute of Material Science Suib, Steven; University of Connecticut, Institute of Material Science

SCHOLARONE™
Manuscripts

Journal Name

RSCPublishing

ARTICLE

Superhydrophobic and Stable Mesoporous Polymeric Adsorbent for Siloxane Removal: D4 Super-Adsorbent

Cite this: DOI: 10.1039/x0xx00000x

Received 00th January 2012,
Accepted 00th January 2012

DOI: 10.1039/x0xx00000x

www.rsc.org/

Tahereh Jafari,[a]‡ Iman Noshadi,[b,c]‡ Nasser Khakpash [a] and Steven L. Suib* [a,d]

Synthesis of a new class of siloxane adsorbent (D4) was done to purify methane-rich gases including biogas and digester gas, at near ambient temperature and atmospheric pressure. The nanoporous polymeric adsorbent with controlled wettability was successfully prepared under solvothermal conditions. Imidazole groups were introduced into the samples by copolymerization of divinylbenzene (DVB) with 1-vinylimidazole (VI). The copolymer composition was varied to obtain optimum adsorption performance. Low-cost PDVB and PDVB-VI were evaluated under different adsorption conditions with a gas flow rate of 10mL/min. To simulate near real time biogas composition, 50%-relative humidity at 25°C was maintained to assess the effect of humidity on D4 removal efficiency. In addition, the mixture gas was used to evaluate the adsorptive activity in the presence of CO_2 (up to 35%). While PDVB alone demonstrates a significant adsorption activity with a capacity of 1951±74 mg/g, an improvement in adsorption capacity to 2370±92 mg/g, was noted with PDVB-VI. Characterization of exhausted adsorbent demonstrates the correlation between D4 adsorption and PDVB-VI-x textural properties. Finally, PDVB-VI-x was readily regenerated after five cycles with less than 10% loss in adsorption activity under both dry and humid conditions.

Introduction

Volatile organic silicon compounds including siloxanes are one of the biggest challenges in the utilization of biogas to generate energy. Micro-organisms in the absence of air produce biogas by anaerobic metabolism[1] which contains traces of various adverse compounds (Table S1 shows the biogas detailed composition[2]). During siloxane combustion in engines, an abrasive microcrystalline silicon oxide gets deposited that prohibits indispensable heat conduction and lubrication[3, 4]. Consequently, biogas combustion without siloxane purification leads to considerable damage to the energy recovery systems (Table S2 is a summary of both linear and cyclic siloxanes and their properties). In the landfills, large molecule siloxane such as D6 may decompose to smaller molecules such as D4 or D5, which volatilizes easily to make biogas with siloxane concentrations of one to ten parts per million (ppm) (v/v)[5]. However, the amount of siloxane should be kept under one part per million (ppm) to meet the limitation of manufacturers of energy recovery systems (0.03-28mg/m^3)[6]. Therefore, biogas refining becomes an indispensable process to prevent high annual costs of maintenance and renovation of micro-turbines, internal combustion engines, fuel cells, and boilers.

The reason for a considerable amount of siloxane in sewage gases is the extensive applications of siloxane-contained compounds such as personal care products, pharmaceuticals, lubricants, adhesives, elastomeric usage and heat-transfer fluids[5, 7] which is due to the favourable properties of siloxane including high compressibility, low surface tension, low allergy causing, low toxicity, and low flammability.

Recent techniques have been applied to remove siloxane from biogas including absorption[8], bio-filtration[9], adsorption[10], peroxidation[11], cryogenic separation[12], membrane filtering[13] and catalytic processing[14]. Siloxane capture by the adsorption method is the most widely used technique over several solid adsorbents[15-19]. However, developing siloxane elimination is expensive which merits intense research on the development of a new class of inexpensive, highly stable adsorbents with large adsorptive capacity and good regenerability.

Siloxane removal from biogas and sewage gases has been investigated using several types of inorganic adsorbents including silica[16], alumina[20], activated carbons or activated charcoal (ACs)[21] and organic adsorbents such as amorphous organic polymer[15], Tenax, and Amberlite[22]. Although they have shown activity toward siloxane capture, most of them have relatively low capacity (100-400mg/g) and poor regenerability. However, some of ACs have revealed interesting adsorption

capacities (800-1700mg/g), so they have been extensively used to remove siloxane contaminants with the advantage of their high surface areas and large pore volumes[5, 10] (Table S3 represents a few of the various very recent adsorbents with their maximum capacity reported up to now[5, 17, 23]).

Although many ACs are commercially applied as adsorbents, comprehensive regeneration of ACs after capturing siloxane remains a challenge. Strong binding between adsorbate and adsorbent[19] or polymerization of siloxane on the surface of AC[5] could be an explanations. Co-adsorption of siloxanes and water (under humid conditions) decreases adsorption performance of ACs because of partial hydrophilicity.

Some porous polymers have shown enormous potential in the area of adsorption of different organic molecules such as dyes and oils[24]. Polymers can be modified readily by a functional group to develop adsorptive properties. Another interesting feature of polymeric structures is the potential of becoming hydrophobic[25] by varying the copolymer type or becoming hydrophilic[26] with loaded heteroatoms (such as LiCl) which makes such materials applicable as a humidity sensor. The synthesis of a hydrophobic material with high adsorption properties for organic molecules removal is necessary to solve current problems in biogas purification technology. PDVB has been synthesized in many structures such as microspheres[27], macroporous monoliths[28], and mesoporous[24-26, 29] structures for diverse applications including water treatment[24], humidity sensing[26], benzoin condensation[25] and adsorption[29].

In this study, we examined the selective capture of siloxane by several PDVB adsorbents, with the focus on the removal of octamethylcyclotetrasiloxane (D4, Figure S1) which is highly abundant in biogas. The synthesis of nanoporous polymer was done by copolymerization of monomers of DVB and 1-vinylimidazole (PDVB-VI-x, where x stands for the molar ratio of DVB over VI) under solvothermal conditions. An investigation on improvement of porous PDVB was conducted with the objective of copolymer incorporation into the polymer structure for siloxane capture.

The superhydrophobic adsorbents perform as novel sorbents and possess abundant nanopores, good air-stability and super wettability for siloxane removal, which results in their very high adsorption capacities. High surface area and large pore volume of PDVB-VI-x leads to effective routes to efficient and stable adsorbents, which is important for the wide applications of solid bases in adsorption industry.

Experimental

Materials and Methods

Synthesis of Imidazole Functionalized-PDVB. Divinylbenzene (technical grade, 80%) 1-Vinylimidazole (VI) (99%), 2,2′-Azobis(2-methylpropionitrile) (AIBN), Ethyl acetate (EtoAC) and Tetrahydrofuran (THF) were purchased from Sigma-Aldrich. Solvents and materials were used as received. Imidazole functionalized nanoporous polymers of PDVB-VI-x were solvothermally synthesized from the copolymerization of DVB with VI (as shown in Figure 1), which was achieved with DVB/VI at molar ratios in the range of 1/0.5 to 1/0.12. In a typical experiment, 2.0g of divinylbenzene (DVB) and 0.74g of VI were added into a solution containing 0.0625g of azobisisobutyronitrile (AIBN) and 30mL of ethyl acetate. After stirring at room temperature for 3h, the mixture was transferred into an autoclave and heated at 100°C for 24h. After slowly evaporating the solvent at room temperature for 2 days, the solid with monolith morphology designated as PDVB-VI was obtained. For comparison, PDVB was synthesized according to the literature[24, 26]. In a typical synthesis, 2g DVB was dissolved in 20mL tetrahydrofuran (THF) with 0–2mL deionized water, and then 0.05g AIBN was added. After stirring for 4h at room temperature, the solution was placed in an autoclave and then treated at 60–100°C for 24h. The system was cooled to room temperature and a solid monolith completely dried was obtained after the slow evaporation of the solvent.

Materials Characterizations. Nitrogen adsorption desorption isotherms were obtained using a Micromeritics ASAP 2020M system. The samples were outgassed for 10h at 150°C before the measurements. The pore size distribution of the samples was calculated using the Barrett–Joyner–Halenda (BJH) model. Fourier transform infrared spectroscopy (FTIR) spectra were recorded by using a Bruker 66V FTIR spectrometer. Thermo-gravimetric analyses (TGA) were achieved on a Perkin-Elmer TGA7 with a heating rate of 10°C/min. Scanning electron microscopy (SEM) images were performed on JSM-6700F electron microscopes. Contact angles were obtained with a DSA10MK2G140 instrument, Kruss Company, Germany.

Adsorption Process. A nitrogen stream passes through two separate bubblers containing D4 and water (in the case of having relative humidity). ALICAT mass flow controllers control the flow rate. Then the gas passes through the adsorbent bed, which is fixed with glass wool at the two ends of a tube with dimensions of 0.25-inch diameter and 7.0-inch length. The gas stream was finally trapped by a hexane solution, which is placed in an ice-bath (the schematic view of a homemade set up that was used for D4 adsorption, is displayed in Figure S2). A blank run was conducted with only glass wool in the tube (no adsorbent). The amount of siloxane in the trap was determined using gas chromatography mass spectroscopy (GC/MS), GCMSD-5975 from Agilent (Single quad spectrometer with a Quadrex 007-5-15-0.33F column) for a limited length of time (3h). Then for each adsorbent GC, which is calibrated based on standard solutions of siloxane (Figures S3, S4 and S5 show the GC patterns of standard solutions for D4 in the trap for PDVB-VI-x and AC respectively), evaluated the amount of D4 in hexane. The difference between siloxane in the trap for the blank run and adsorbent loaded one would be the adsorbed D4 on the adsorbent bed. GC (with split ratio of 20:1) detects D4 by auto-sampler injection. In the adsorption process, our material was compared with the widely used commercial activated charcoal (AC) purchased from Sigma-Aldrich.

Results

Characterization of Fresh Adsorbent

Scanning Electron Microscopy (SEM). Figure 2 showed the electron microscopic images of PDVB and PDVB-VI. SEM images (Figure 2A and B) showed that PDVB and PDVB-VI have a rough surface with abundant nanopores. Given the pore size, ranged 5-100 nm, this is in agreement with N_2 isotherms results (Figure 3). The electron microscope images indicated

 This journal is © The Royal Society of Chemistry 2012

that PDVB and PDVB-VI exhibit a hierarchically nanoporous structure, ideal for facilitating fast diffusion, which further results in their high exposition degree of adsorption.

Brunauer–Emmett–Teller (BET) Isotherm. Figure 3 shows the N_2 adsorption-desorption isotherms of PDVB and PDVB-VI-x. For all PDVB samples, Type IV curves were observed with a sharp capillary condensation step at a relative pressure of P/P_0 = 0.7–1.0, indicating the presence of abundant mesopores in these samples[30]. Additionally, all porous PDVB have large BET surface areas in the range of 594 to 830 m^2/g and uniform pore diameters centred at 25.3 to 15.97 nm were observed. Additionally, the changes in total pore volume are relatively linear because of VI addition. At a very low amount of copolymer (x=0.12), total pore volume increased from 1.66 to 1.75cc/g by incorporation of VI to PDVB structure. Further copolymerization reduces the total pore to 1.16cc/g. Large surface area, uniform large pore sizes, and high pore volume were the factors behind their superior adsorption performances.

Fourier Transform Infrared Spectroscopy (FTIR). Figure 4 showed PDVB, PDVB-VI infrared peaks. In the FTIR characterization, the reflectance mode was used. Comparing PDVB-VI to PDVB, peaks around 1679, 1280 and 1226 cm^{-1} associated with C-N and C=N species indicate successful incorporation of the imidazole group into the network of the porous polymer to make PDVB-VI[31]. Vinylimidazole underwent radical polymerization along with the DVB to form a copolymerized and cross-linked network comprising the two co-monomers in PDVB-VI.

Contact Angle Measurement. Figure 5 shows the water contact angle of PDVB and PDVB-VI, which indicate their hydrophobicity. A water droplet, in contact with PDVB yielded a contact angle up to 156° (Figure 5a), indicating its super-hydrophobic character. In the sample of PDVB-VI-0.5, the water contact angle was 148° (Figure 5b). While there was a small drop in the water contact angle with PDVB-VI-0.5, this value is still high enough for the sample to exhibit excellent hydrophobicity.

Thermo Gravimetric Analysis (TGA). Figure 6 shows the thermal stability of PDVB-VI-x mesoporous polymers. Both types of PDVB (with and without imidazole group incorporation) have good thermal stability in which less than 3% weight loss was observed up to 400°C, which may relate to remained solvent in the polymer.

Characterization of Spent Adsorbent

In figure 7, the FTIR spectrums of the PDVB-VI before and after adsorption are shown. The qualitative analysis of siloxane D4 in the PDVB-VI can be performed by following the intensity of the bands at 1074 and/or 810 cm^{-1}, which may be ascribed to the asymmetric and symmetric stretching of the Si-O-Si siloxane bridge bonds of siloxane D4. The Si-CH_3 bond can be seen clearly at 1261 cm^{-1}. Furthermore, the TGA result (Figure 8) confirms the huge adsorption of D4 by our material, which shows rapid weight loss (67%) of PDVB-VI-0.5 after exhaustion in the temperature range of 25 to 100°C, which is in the range of D4 decomposition.

To investigate the exhausted PDVB-VI textural changes, solid-state ^{29}Si NMR measurements were carried out (Figure 9). While there is no Si peak in the porous adsorbent prior to adsorption, a bulk siloxane-D4 peak appears at -19.2ppm after adsorption showing the adsorption and possible entrapment of the siloxane inside the porous adsorbent structure.

Figure 10 shows the BET isotherms for the adsorbent before and after D4 capture. The surface area of the adsorbent, shown as (a), is computed to be 594m^2/g, which reduced to 72m^2/g after several hours of exposure to the adsorbent, shown as (b) and then to 0m^2/g after complete saturation, shown as (c). This demonstrated that the siloxane keeps filling up the pores of the porous adsorbent until a saturation point is reached wherein no more adsorption can take place.

The average pore volume, after adsorption is reduced to 0.76cc/g after three hours of exposure to the high concentration of siloxane. After the saturation, pore volume is reduced to a level that was below the computation capability of the instrument. This indicates there are probably multiple adsorption and entrapment sites inside each pore, which fill up gradually as indicated by the gradual decrease in the average pore size. This continues until the pores can accommodate no more siloxane moieties and becomes unavailable for further adsorption.

Adsorption Curves under Dry Condition. In order to obtain the adsorptive activity of PDVB-VI-x in comparison with available commercial AC, 10sccm of nitrogen flow was bubbled in D4, which passes through the adsorbent bed. A flow rate of 10sccm provides an even higher amount of D4 than real concentration of siloxane in the biogas. Figure 11 shows the adsorptive activity of PDVB-VI samples in comparison with commercial AC. None of PDVB-VI-x was exhausted during the adsorption process. Similarly, commercial AC does not show failure of adsorption under the same condition. (Figure S3 displays GC pattern of D4-standard solutions, which are used for calibration).

Adsorption Curves under Humid Condition. As biogas usually contains moisture, it is important to consider this kind of harsh condition during the adsorption process. The nanoporous PDVB-VI-x materials were assessed under moisture conditions with a relative humidity (RH) of 50%. Figure 12 illustrates that commercial AC starts to breakthrough after 100min, which indicates its earlier failure in compare with PDVB-VI.

When RH was increased, PDVB-VI samples still adsorbed all D4 in the gas stream (similar to dry condition, no exhaustion was observed). This activity might be attributed to the superhydrophobicity of PDVB materials that leads to its high activity even under wet conditions. While commercial AC adsorption performance reduces under humid environment, PDVB-VI-x not only has a high ability to capture D4, but also overcomes the limitation of deactivation of ACs by water vapour. (Figure S4 and S5 shows the GC patterns of PDVB-VI-x and AC under humid condition respectively).

Adsorption Curves under Mixed Gas. Presence of CO_2 may change the adsorption performance of siloxane because of its high concentration (up to 35% (vol-%)). The nanoporous PDVB-VI-x materials were evaluated under the mixture of CO_2 and siloxane (35% CO_2). Figure 13 displays no exhaustion of PDVB-VI-x and commercial AC under a gas mixture of CO_2. However, the commercial AC shows less activity toward siloxane capture than PDVB-VI-x.

Capacity Determination. To calculate the capacity (mg-D4/g-adsorbent), the solid adsorbent was saturated by siloxane with continuous gas flow for 17h (100sccm). The exhausted adsorbent was washed off by hexane and then the solvent was tested by GC/MS to evaluate the amount of captured D4. (Figure S6 shows the GC pattern of washed PDVB-VI and AC).

As mentioned before, synthesized PDVB contains about 3% solvent residue (THF), which may have an effect on adsorption performance of the material. So, the heat-treated PDVB at temperatures higher than the boiling point of solvent (70°C) for 24 h (PDVB-HT) undergoes the capacity measurement which shows similar results to that of PDVB (Table S4).

Table 1 shows textural and adsorptive comparison of commercial AC and PDVB-VI-x (x=0-0.5). PDVB-VI-x actively remove D4 as a non-precedent "super-adsorbent" which may markedly help the problematic issue related to the utilization of biogas. Such a huge capacity for siloxane removal has not been reported to date.

Table 1, also explains the effect of the copolymer (VI) addition to the PDVB structure simultaneously, revealing the moisture resistance of PDVB-VI-x. Addition of the copolymer in the synthesis of PDVB-VI enhanced the adsorption performance of the material at an optimum level of VI. As the amount of VI increased in the x ratio to 0.12, the adsorption behaviour improved. However, further enhancement of x to 0.24 and 0.50 declined the adsorption activity in comparison with PDVB.

Table 2 displays a comparison of adsorptive performance of PDVB-VI-0.12 under two different gas compositions. These data indicate that the presence of CO_2 has not reduced the adsorption capacity but has elevated the capacity to about 25%. Interestingly, CO_2 hinders the saturation of PDVB-VI, which needs further in depth investigation.

Effect of the PDVB-VI-x Textural Properties on D4 Capture. Figure 14 shows the correlation of the adsorptive capacity with BET surface area and total pore volume data. Figure 14a indicated that for the imidazole incorporated to PDVB, surface area controls the adsorption performance at both low and high amounts of the copolymer. Overall, there is a relatively good relationship between D4 capture and the surface area of PDVB-VI-x. Additionally, there is a good correlation between adsorptive capacity and total pore volume (Figure 14b). The addition of the copolymer at a specific level reduces the surface area in comparison with PDVB. However, copolymerization still leads to a high total pore volume, which controls the adsorption procedure. As the cross sectional size of D4 molecule is reported to be 1.08×1.03nm[32], larger pore volumes are expected to capture more D4 molecules. Consequently, a higher pore volume is more relevant to D4 adsorption. These results are in agreement with literature reports on textural behaviour of various ACs[5].

Adsorbent Regeneration. Not only does the adsorbent need to have high capacity of adsorption under dry and humid mixture conditions, but its capacity also needs to remain the same after being exhausted repeatedly. For the developed super-adsorbent PDVB-VI-0.12, the reusability was tested under dry and moist conditions (Figure 15). For regeneration, the adsorbent was heated to 100°C in air overnight. This showed that PDVB-VI is able to adsorb almost the same amount of siloxane with less than 5% loss in capacity. It indicates that siloxane molecules are not tightly bonded to PDVB-VI because of its ease-recovery at low temperatures. However, ACs were hardly recovered at higher temperatures (250-300°C) for a longer period of time[19] which might be related to the polymerization of D4 on the surface of ACs suggested by Cabrera-Codony due to the phenolic and carboxylic on its surface[5]. Readily regenerated PDVB-VI might be an indication that such a phenomenon could not occur for this mesoporous polymer since D4-polymerization hinders the thermal regeneration process.

Conclusions

This study suggests a new type of organic D4 adsorbent, which has not been reported up to now. PDVB with a very simple and inexpensive synthesis procedure, showed great adsorption performance, even well than the best ACs reported to date[5]. High surface area and large total pore volume make this mesoporous polymer an efficient siloxane adsorbent. PDVB with Imidazole group incorporation (PDVB-VI-x) opens a new path in the utilization of biogases for energy generation. This work indicates that an optimum amount of copolymer ratio to primary monomer (x=0.12) enhanced the adsorptive capacity of PDVB which also shows a good regenerability at low temperatures. Investigation of textural properties of PDVB-VI reveals that total pore volume is the key parameter in siloxane capture. The PDVB-VI-x activity toward siloxane has not been significantly influenced by the presence of moisture. However, the presence of CO_2 has interestingly enhanced the adsorption performance of PDVB-VI, which will be explored in the future. In conclusion, development of nanoporous PDVB-VI may open new vistas for the manufacture of more efficient and stable adsorbents with wide potential industrial applications.

Acknowledgements

We acknowledge the support of the Center of Energy Innovation of the UCONN Fraunhofer Institute for support of this work.

Notes and references

[a] Institute of Materials Science, University of Connecticut, U-3060, 91 North Eagleville Road, Storrs, Connecticut 06269, United States

[b] Department of Chemical & Biomolecular Engineering, 191 Auditorium Road, Unit 3222, Storrs, CT 06269-3222, United States

[c] Harvard-MIT Health Sciences and Technology, Massachusetts Institute of Technology, 77 Massachusetts Ave, Cambridge, MA 02139, United States

[d] Department of Chemistry, University of Connecticut, U-3060, 55 North Eagleville Road, Storrs, Connecticut 06269, United States s here.

‡These authors contributed equally.

*Correspondence and requests for materials should be addressed to S.L.S. (email:steven.suib@uconn.edu).

Electronic Supplementary Information (ESI) available: [details of any supplementary information available should be included here]. See DOI: 10.1039/b000000x/. Biogas composition at the entrance of the biogas polishing system at 30°C and 25-30mbar (Table S1), properties of linear and cyclic siloxanes (Table S2) and some high capacity current alternative for siloxane removal (Table S3), the siloxane adsorption capacity of PDVB and PDVB-HT (Table S4). Molecular configuration of D4 (Figure S1), schematic view of siloxane adsorption set-up (Figure S2), GC/MS pattern of standard concentration of D4 in hexane which was used to derive calibration curve (Figure S3), GC/MS pattern of amount of D4 in trap which was sampled at different time interval when PDVB-VI-x under 50% RH was loaded (Figure S4), GC/MS pattern of amount of D4 in trap which was sampled at different time interval when AC under 50% RH was loaded (Figure S5) and GC/MS pattern of saturated AC and PDVB-VI-x, washed by hexane (Figure S6).

 This journal is © The Royal Society of Chemistry 2012

1. E. Ryckebosch, M. Drouillon and H. Vervaeren, *Biomass. Bioenerg.*, 2011, **35**, 1633.
2. N. de Arespacochaga, C. Valderrama, C. Mesa, L. Bouchy and J.L. Cortina, *Chem. Eng. J.*, 2014, **255**, 593.
3. N. Nair, A. Vas, T. Zhu, W. Sun, J. Gutierrez, J. Chen, F. Egolfopoulos and T. Tsotsis, *Ind. Eng. Chem. Res.*, 2013, **52**, 6253.
4. N. Nair , X. Zhang, J. Gutierrez, J. Chen, F. Egolfopoulos and T. Tsotsis, *Ind. Eng. Chem. Res.*, 2012, **51**, 15786.
5. A. Cabrera-Codony, M.A. Montes-Moran, M. Sanchez-Polo, M.J. Martin and R. Gonzalez-Olmos, *Environ. Sci. Technol.*, 2014, **48**, 7187.
6. P. Gilson, S. Galli and G. Monteleon, *Wast. Manage.*, 2013, **33**, 2687.
7. R. Dewil, L. Appels and J. Baeyens, *Energ. Convers. Manage.*, 2006, **47**, 1711.
8. L. Ghorbel, R. Tatin and A. Couvert, *Environ. Technol.*, 2014, **35**, 372.
9. F. Accettola, G.M. Guebitz and R.Schoeftner, *Clean. Technol. Envir.* , 2008, **10**, 211.
10. M. Yu, H. Gong, Z. Chen and M. Zhang, *J. Environ. Chem. Eng.*, 2013, **1**, 1182.
11. L. Appelsa, J. Baeyens and R. Dewil, *Energ. Convers. Manage.*, 2008, **49**, 2859.
12. M. Hagmann, E. Hesse, P. Hentschel and T. Bauer, in *The eighth international waste management and landfill symposium*, eds. T. H. Christensen, R. Cossu and R. Stegmann, Litotipografia Kalb, Cagliari, Italy, 2001, vol. II, pp. 641.
13. M. Ajhar and T. Melin, *Desalination*, 2006, **200**, 234.
14. L. Lamaa, C. Ferronatoa, S. Prakasha, L. Finea, F. Jaberb and J.M. Chovelon, *Appl. Catal. B-Environ.*, 2014, **156-157**, 438.
15. Y. Mito-oka, S. Horike, Y. Nishitani, T. Masumori, M. Inukai, Y. Hijikata and S. Kitagawa, *J. Mater. Chem. A*, 2013, **1**, 7885.
16. L. Sigot, G. Ducom, B. Benadda and C. Labouré, *Fuel*, 2014, **135**, 205.
17. E. Finocchio, T. Montanari, G. Garuti, C. Pistarino, F. Federici, M. Cugino and G. Busca, *Energ. Fuel.*, 2009, **23**, 4156.
18. T. Montanaria, E. Finocchio, I. Bozzano, G. Garuti, A. Giordano, C. Pistarino and G. Busca, *Chem. Eng. J.*, 2010, **165**, 859.
19. M. Ajhar, M. Travesset, S. Yücea and T. Melina, *Bioresource Technol.*, 2010, **101**, 2913.
20. E. Finocchio, G. Garuti, M. Baldi and G. Busca, *Chemosphere*, 2008, **72**, 1659.
21. B. Boulinguiez and P.L. Cloirec, *Energ. Fuel.*, 2010, **24**, 4756.
22. M. Schweigkofler and R. Niessner, *J. Hazrd. Mater. B*, 2001, **83**, 183.
23. S. Giraudet, B. Boulinguiez and P. Le Cloirec, *Energ. Fuel.*, 2014, **28**, 3924.
24. Y. Zhang, S. Wei, Y. He, F. Nawaz, S. Liu, H. Zhang and F. Xiao, *J. Mater. Chem.*, 2010, **20**, 4609.
25. D. Kuzmicz, P. Coupillaud, Y. Men, J. Vignolle, G. Vendraminetto, M. Ambrogi, D. Taton and J. Yuan, *Polymer*, 2014, **55**, 3423.
26. T. Fei, K. Jiang, S. Liu and T. Zhang, *Sensor. Actuat. B-Chem.*, 2014, **190**, 523.
27. F. Bai, X. Yang and W. Huang, *Macromolecules*, 2004, **37**, 9746.
28. K. Kanamori, K. Nakanishi and T. Hanada, *Adv. Mater.*, 2006, **18**, 2407.
29. X. Feng, C. Gao, Z. Gua, Y. Zhou and J. Wang, *R. Soc. Chem. Adv.*, 2014, **4**, 23389.
30. Y. Zhang, S. Wei, F. Liu, Y. Du, S. Liu, Y. Ji, T. Yokoi, T. Tatsumi and F.S. Xiao, *Nano Today*, 2009, **4**, 135.
31. F. Liu, R.K. Kamat, I. Noshadi, D. Peck, R.S. Parnas, A. Zheng, C. Qi and Y. Lin, *Chem. Commun.*, 2013, **49**, 8456.
32. J.L. Hamelink, P.B. Simon and E.M. Silberhorn, *Environ. Sci. Technol.*, 1996, **30**, 1946.

Journal Name RSCPublishing

ARTICLE

Table 1. Adsorption capacity of commercial AC and PDVB under dry and moisture conditions for various amounts of copolymer.

Materials	Surface area (m^2/g)	Pore volume (cc/g)	Capacity (GC) (mg/g) RH=0	Capacity (GC) (mg/g) RH=50%
Commercial AC	695	0.52	856±54	547±83
PDVB	831	1.66	1951±74	1940±32
PDVB-VI-0.12	780	1.75	2370±92	2360±50
PDVB-VI-0.24	670	1.3	1586±71	1582±38
PDVB-VI-0.50	594	1.15	1384±62	1381±40

This journal is © The Royal Society of Chemistry 2013

Table 2. Adsorption capacity of PDVB-VI-0.12 with and without CO_2 in the gas stream.

Materials	Regular gas stream	Gas stream with 35%CO_2
PDVB-VI-0.12	2370±92	2970±86
Commercial AC	856±54	480±59

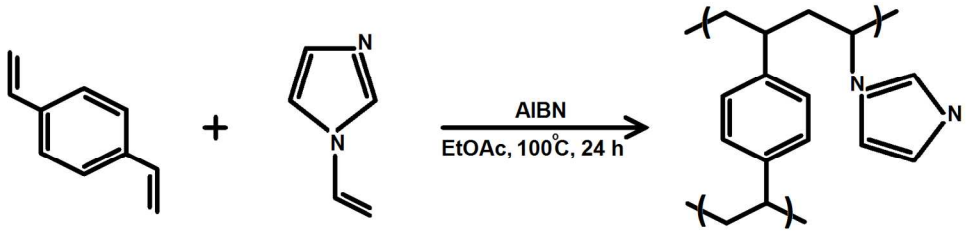

Figure 1. Synthesis procedure of nanoporous polymer framework of PDVB-VI-x.

This journal is © The Royal Society of Chemistry 2012

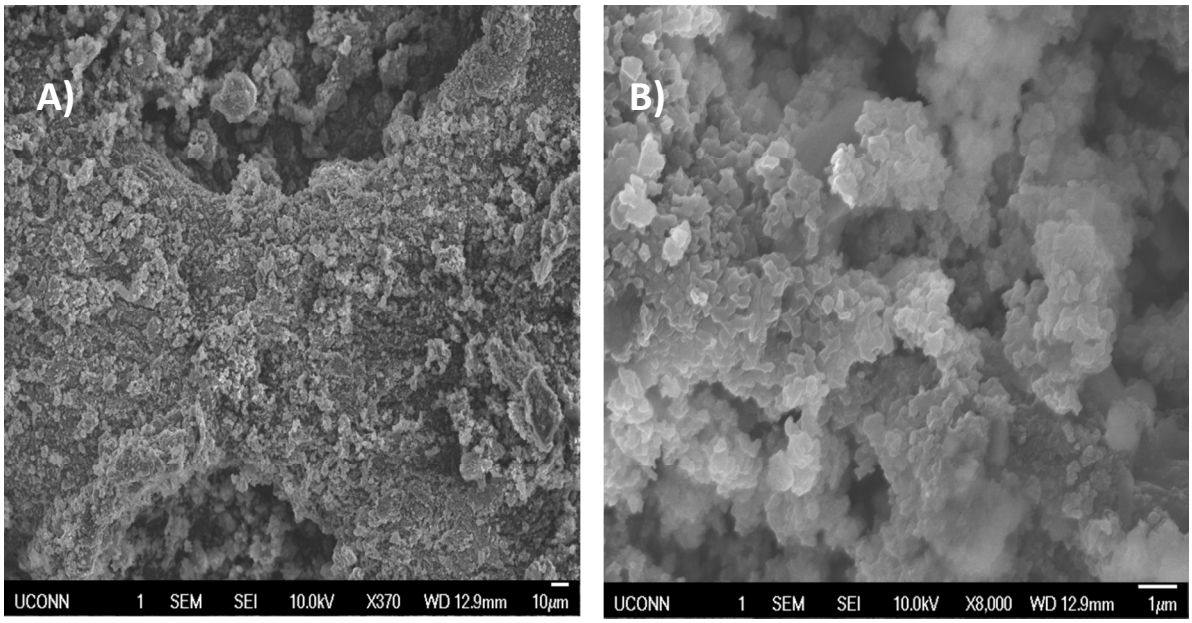

Figure 2. SEM image of PDVB-VI-0.5 A)X370, B)X8000.

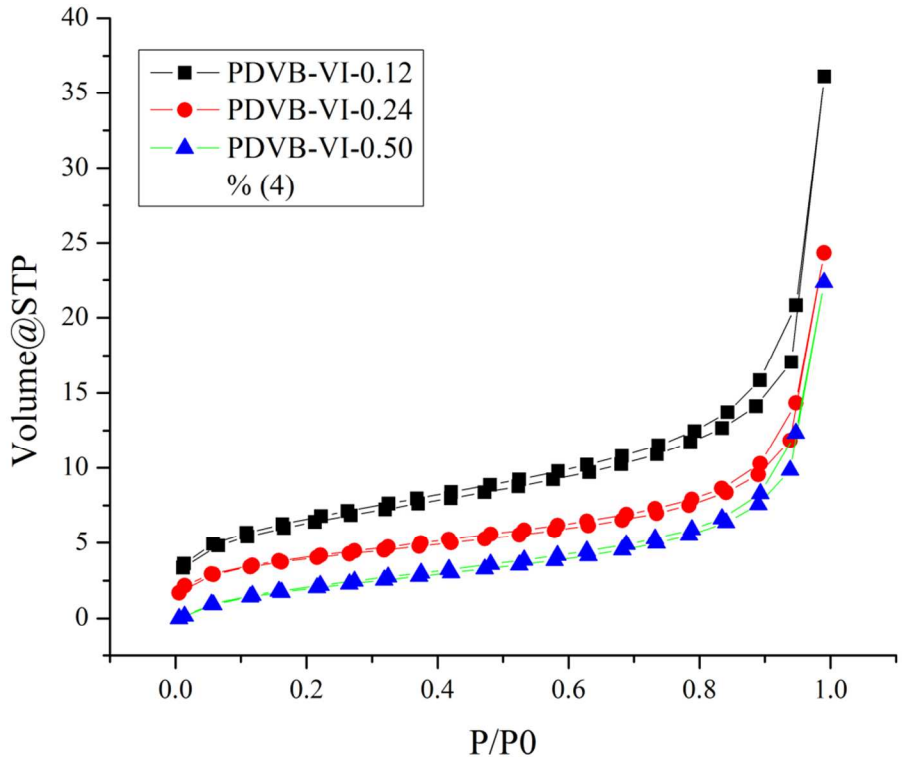

Figure 3. Nitrogen isotherms of PDVB (black), PDVB-VI-0.12 (red), PDVB-VI-0.24 (blue) and PDVB-VI-0.5 (green).

This journal is © The Royal Society of Chemistry 2012

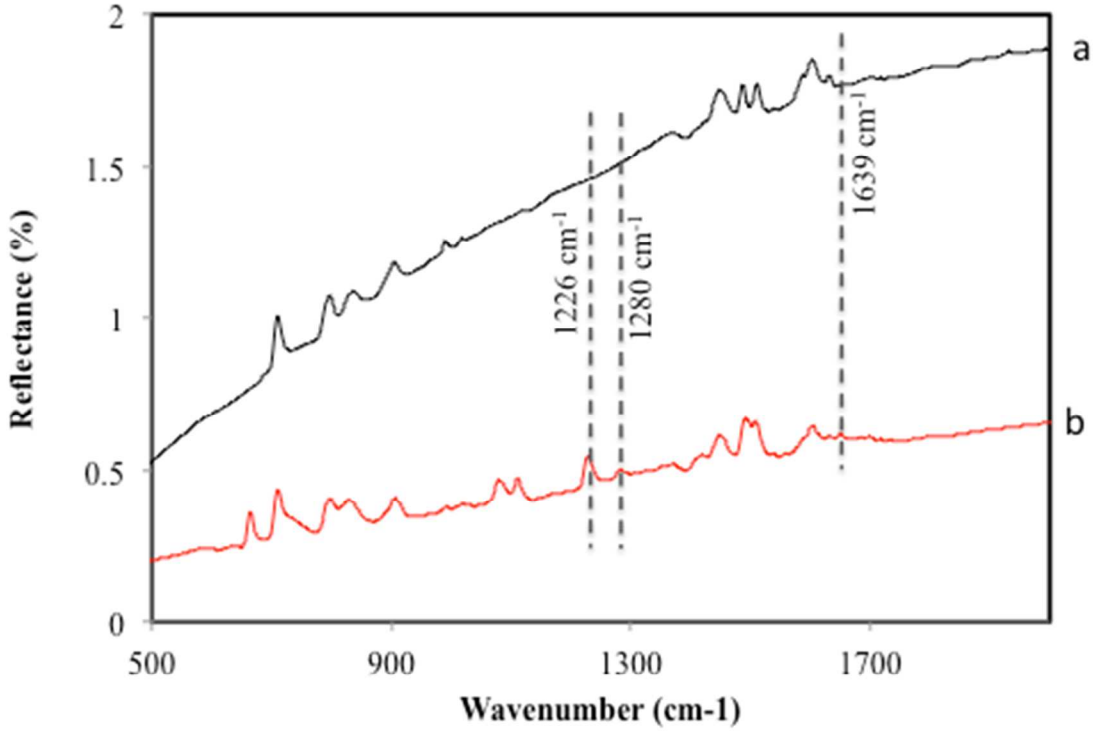

Figure 4. FTIR spectra of a) PDVB and b)PDVB-VI-x (x=0.5).

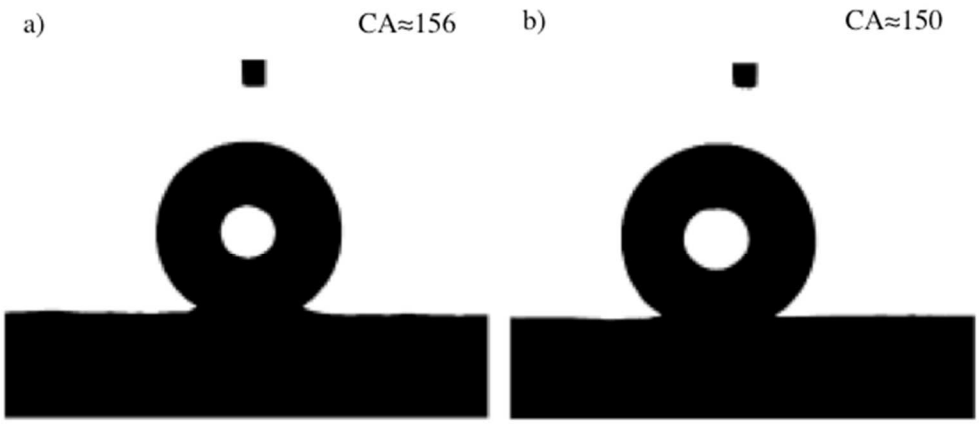

Figure 5. The water contact angle results of a) PDVB and b) PDVB-VI-0.5.

This journal is © The Royal Society of Chemistry 2012

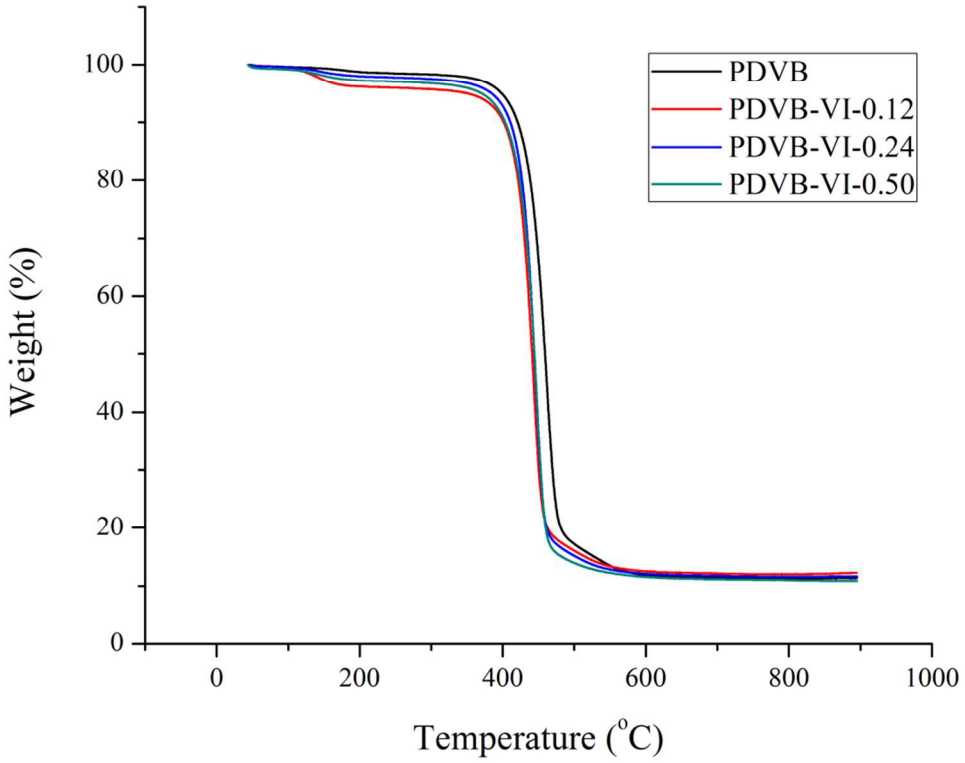

Figure 6. TGA of PDVB and PDVB-VI-x (x=0.12, 0.24, and 0.5).

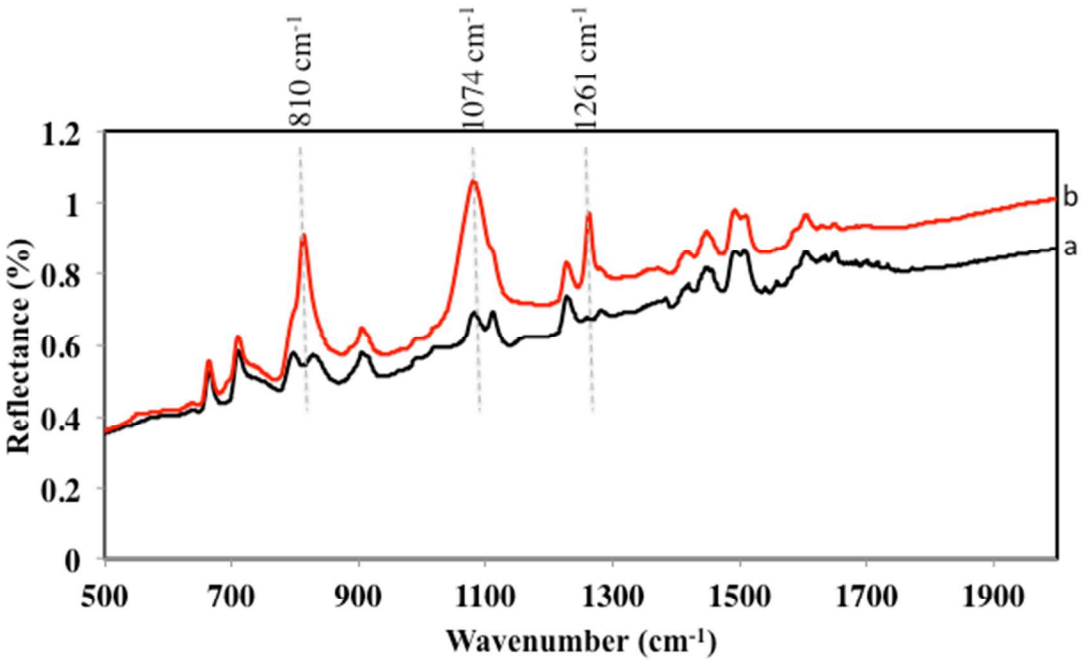

Figure 7. FTIR of PDVB-VI-x before and after adsorption (x=0.5).

This journal is © The Royal Society of Chemistry 2012

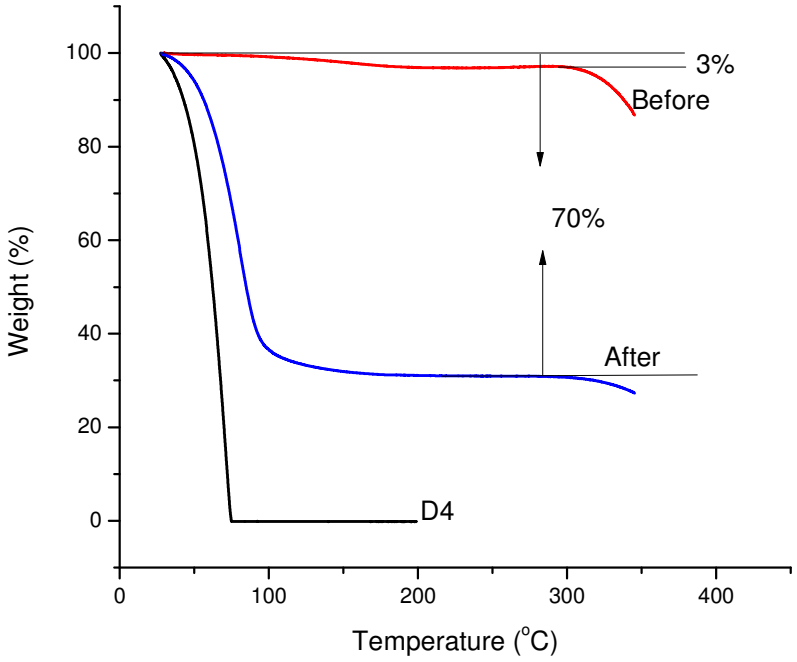

Figure 8. TGA of D4, PDVB-VI-x before and after adsorption process (x=0.5).

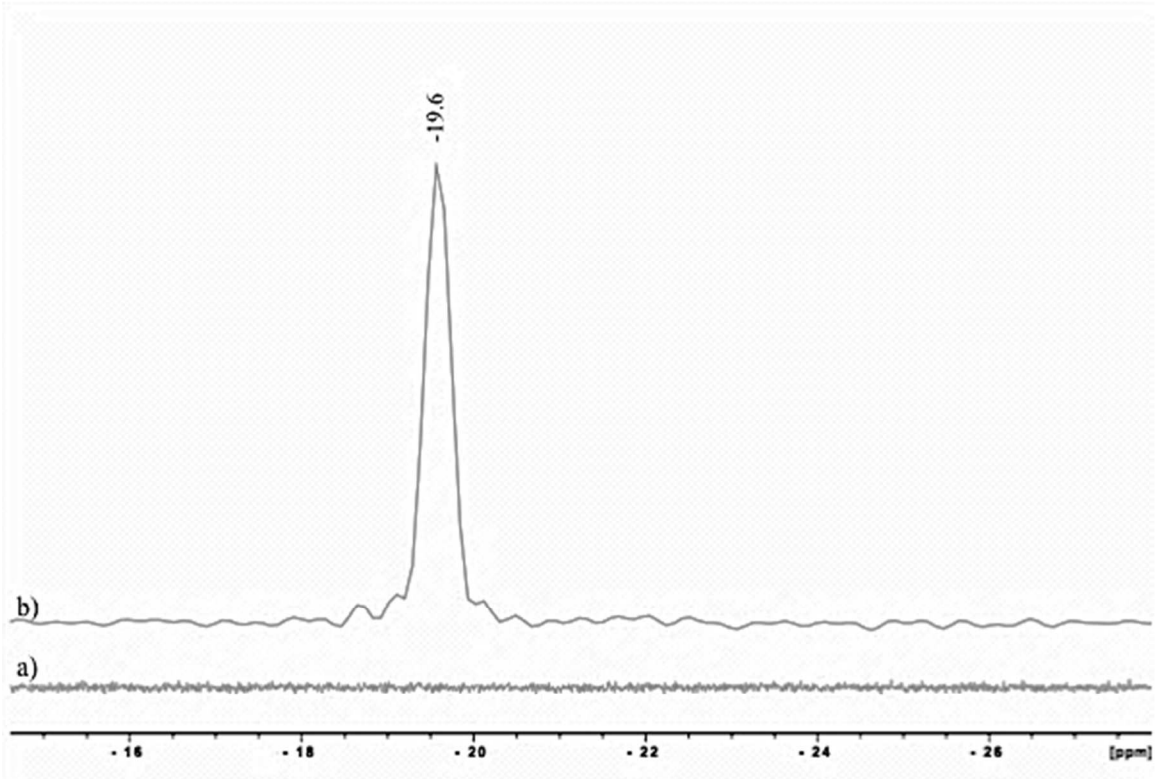

Figure 9. ^{29}Si NMR on PDVB-VI-0.5 a) before and b) after adsorption.

This journal is © The Royal Society of Chemistry 2012

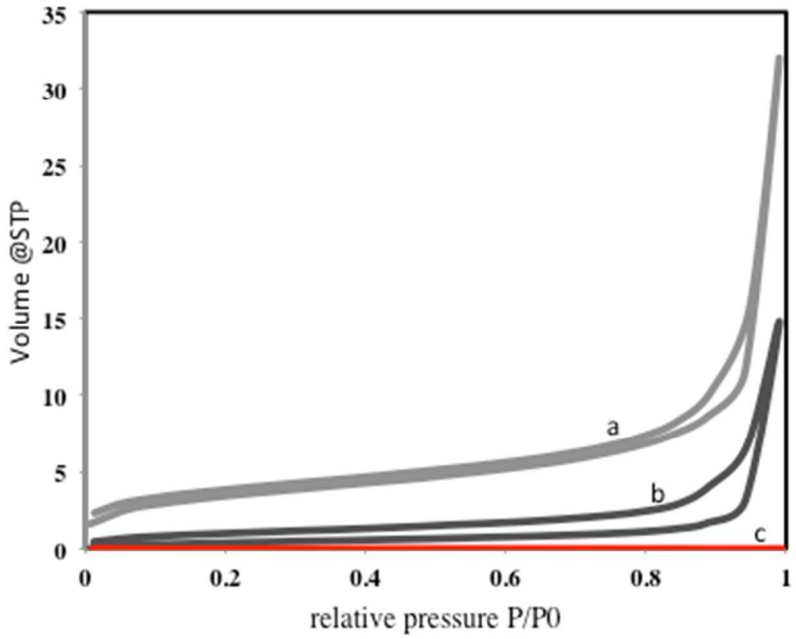

Figure 10. Effect of adsorption on BET surface area of PDVB-VI-0.5, a) before and b,c) after adsorption.

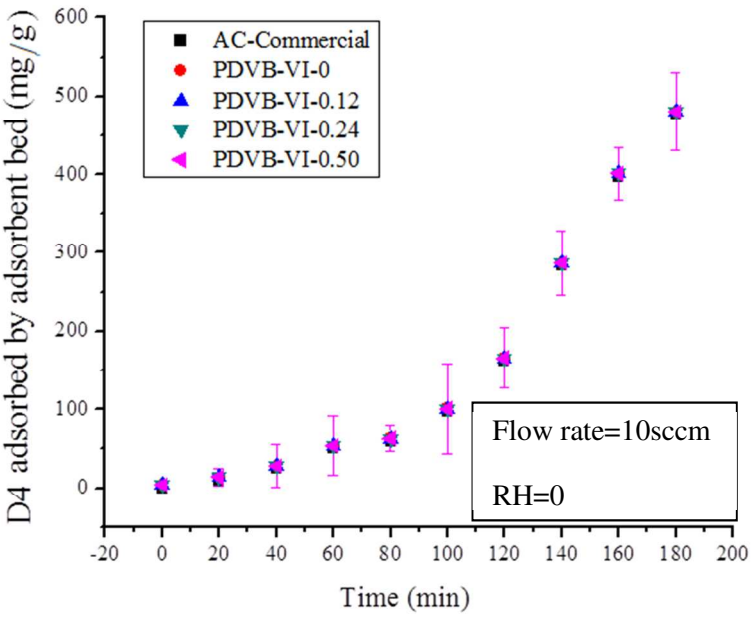

Figure 11. Adsorption activity of AC and PDVB-VI-x under dry conditions with flow rates of 10 sccm (x=0, 0.12, 0.24 and 0.5).

This journal is © The Royal Society of Chemistry 2012

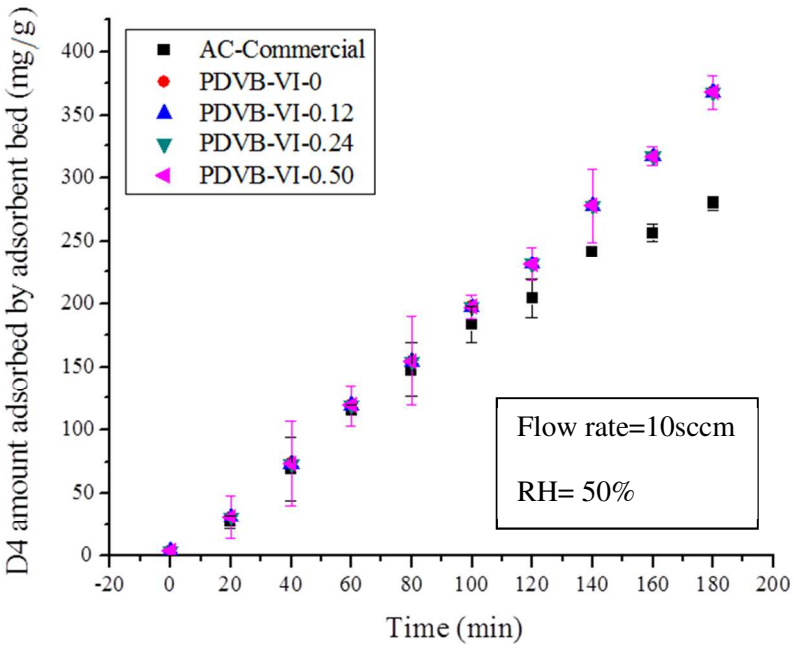

Figure 12. Breakthrough curve (adsorption activity) of AC and PDVB-VI-x at 50% relative humidity and 10 sccm flow rates (x=0, 0.12, 0.24 and 0.5).

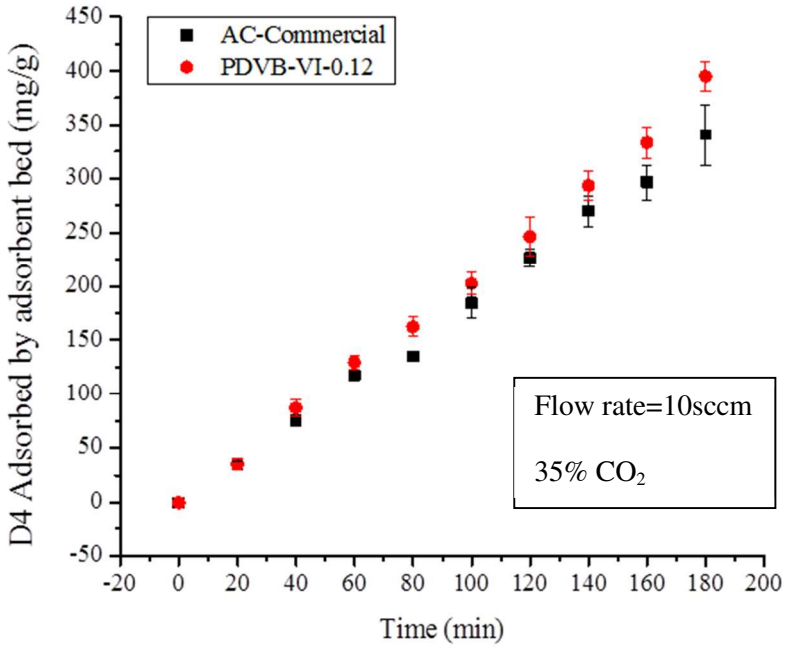

Figure 13. Breakthrough curve (adsorption activity) of AC and PDVB-VI-x under 10 sccm flow of 35%CO_2 (x= 0.12).

This journal is © The Royal Society of Chemistry 2012

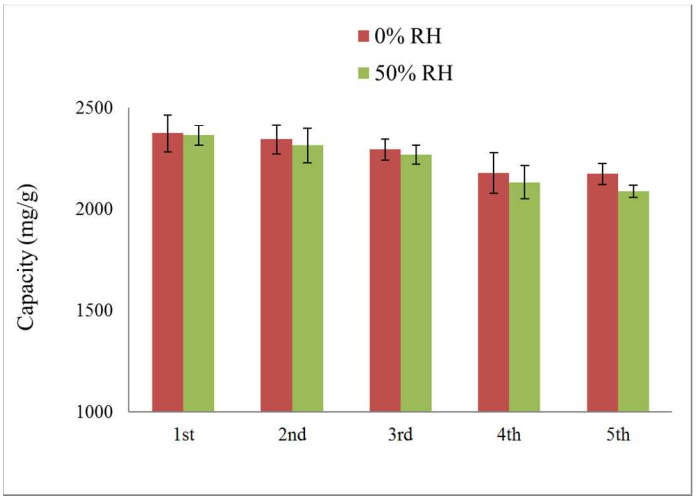

Figure 14. Regeneration of PDVB-VI-x under both dry and moisture conditions (x= 0.12).

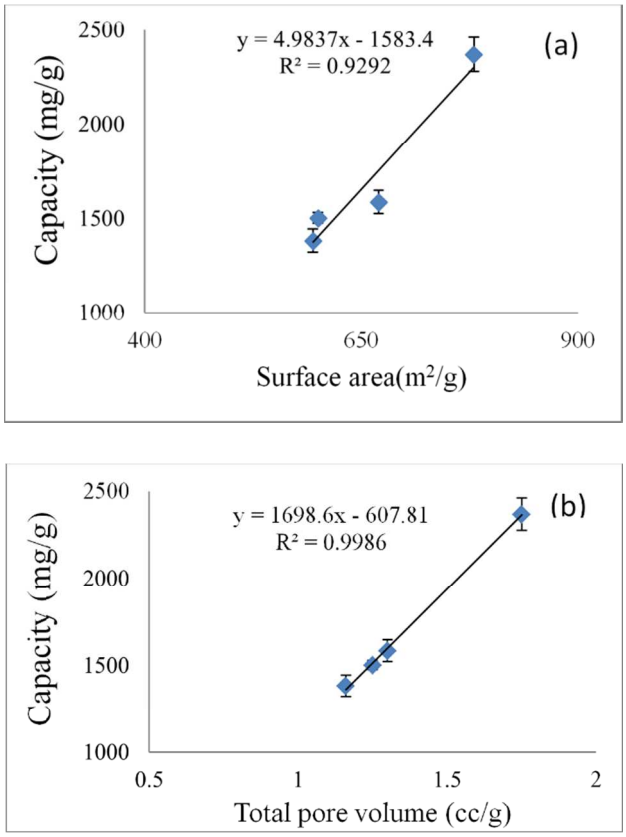

Figure 15. Capacity of PDVB-VI-x in correlation with N_2 adsorption/desorption isotherm data, a) surface area, b) total pore volume.

This journal is © The Royal Society of Chemistry 2012